ACCOUNTING FOR TURBULENCE DESTRUCTION IN THE FLOW OVER FORESTS

A. Silva Lopes
asl@fe.up.pt

J.M.L.M. Palma
jpalma@fe.up.pt

J. Viana Lopes
CEsA – Centre for Wind Energy and Atmospheric Flows
Faculdade de Engenharia da Universidade do Porto
Rua Dr. Roberto Frias, s/n – 4200-465 Porto – Portugal
jvlopes@fe.up.pt

ABSTRACT

Large-eddy simulations of the flow over a long homogeneous forest were used to calibrate the canopy related terms in a RaNS $k-\varepsilon$ turbulence model. It was found that the canopy drag always acts to decrease both the turbulent kinetic energy and its dissipation. The flow across a forest edge was used to see whether the model was also accurate in a more complex flow, with a finite length forest. The effects of the canopy were overestimated in an initial part, but, overall, the accuracy approached the levels found in the case of the long forest.

INTRODUCTION

Flows over forests are of major importance in a large range of applications, including wind energy, forest fires and air pollution. One- and two-equation Reynolds averaged Navier-Stokes (RaNS) turbulence models have been appraised in the prediction of such flows (Katul *et al.*, 2004). However, the development of models for canopy flows still suffers from many deficiencies, one of them being the uncertainty of the model coefficients (Sanz, 2003; Sogachev & Panferov, 2006). By contrast, numerical models using large-eddy simulation (LES) and a drag-force approach for the canopy have been able to reproduce many of the observed features of the flow over vegetation canopies (Shaw & Schumann, 1992; Yang *et al.*, 2006*a*,*b*).

The objective of this work is to use large-eddy simulations and the least squares method to calibrate canopy models for RaNS with $k-\varepsilon$ model. Using LES it is possible to change parameters as the foliage density, which cannot always be varied in field measurements. The model coefficients will be determined mainly using the flow over a long homogeneous canopy. The flow across a forest edge will be used to test the conclusions in a more general configuration.

PROBLEM FORMULATION

Mathematical Model

In LES the fields are separated into resolved (large-scale) and subgrid (small-scale) parts by a spatial filtering operation. The filtered continuity and momentum equations for the velocity field are:

$$\frac{\partial \overline{u}_i}{\partial x_i} = 0 \,, \tag{1}$$

$$\frac{\partial \overline{u}_i}{\partial t} + \frac{\partial (\overline{u}_j \overline{u}_i)}{\partial x_j} = \nu \frac{\partial^2 \overline{u}_i}{\partial x_j \partial x_j} - \frac{\partial \tau_{ij}}{\partial x_j} - \frac{1}{\rho}\frac{\partial \overline{p}}{\partial x_i} + F_i \,. \tag{2}$$

ρ and ν are the standard air density and kinematic viscosity; $\tau_{ij} = \overline{u_i u_j} - \overline{u}_i \overline{u}_j$ are the subgrid stresses, which were modelled using an eddy-viscosity assumption:

$$\tau_{ij} - \delta_{ij}\tau_{kk}/3 = -2\nu_t \overline{S}_{ij} = -2C\overline{\Delta}^2 |\overline{S}| \overline{S}_{ij} \,.$$

Here $\overline{\Delta} = (\overline{\Delta x}\ \overline{\Delta y}\ \overline{\Delta z})^{1/3}$ is the filter size, $\overline{S}_{ij} = \left(\partial \overline{u}_i/\partial x_j + \partial \overline{u}_j/\partial x_i\right)/2$ is the resolved strain-rate tensor and $|\overline{S}| = (2\overline{S}_{ij}\overline{S}_{ij})^{1/2}$ its magnitude. As subgrid model, we used a combination of a wall-damped Smagorinsky near the ground (as in Mason & Thomson, 1992) with, far away, the dynamic model with the Lagrangian averaging technique (Meneveau *et al.*, 1996). Further details about the implementation can be found in Silva Lopes *et al.* (2007).

The canopy model adds an extra term F_i to the momentum equations, which represents the drag force in the x_i direction:

$$F_i = -C_d\, a(z) |\overline{\mathbf{u}}| \overline{u}_i \,. \tag{3}$$

C_d is a drag coefficient, $a(z)$ the leaf area density (LAD) and $|\overline{\mathbf{u}}|$ the resolved scalar velocity, $\left(\overline{u}^2 + \overline{v}^2 + \overline{w}^2\right)^{1/2}$. The leaf

area index (LAI) is generally used to characterize the foliage density and is related to the leaf area density by

$$LAI = \int_0^{h_{\rm can}} a(z)\,{\rm d}z\,,$$

where $h_{\rm can}$ is the canopy height.

Homogeneous Canopy

Physical Domain and Boundary Conditions

The computational domain is identical to Shaw & Schumann (1992) (herein called SS92): a box with 192 m $\times$ 96 m $\times$ 60 m, in the streamwise, spanwise and vertical directions. The forest is located in the lower 20 m of the domain.

Periodic conditions were used in the streamwise and spanwise directions. The wall-model of Marusic *et al.* (2001) was used at the bottom rough surface, with $z_0 = 2$ cm, and a free-slip condition was used at the top surface. To maintain a constant average wind-speed $U_b = 2$ m/s, the streamwise pressure gradient was varied at each time-strep.

Grids SS92 used an isotropic grid with resolution $\Delta x_i = 2$ m ($\Delta x_i/h_{\rm can} = 0.1$). Our initial grid was similar, but refined in the vertical direction near the canopy top, for improved resolution of the strong shear. We found that a resolution $\Delta z_{\rm min} = 0.2$ m was required to avoid oscillations (dispersion error) in the resolved shear $\langle u'w'\rangle$, using a hyperbolic tangent stretching with maximum expansion factor lower than 1.1 and maximum vertical space not much larger than the horizontal ($\Delta z_{\rm max} < 1.1\Delta x$).

A grid refinement study was performed, using the initial (coarse) grid, a fine grid, with twice the resolution in every direction, and a medium grid, with intermediate resolution (table 1).

Table 1. Homogeneous canopy grid resolution. Δx, Δy and $\Delta z_{\rm min}$ in meters; $f_{z_{\rm max}}$ is the maximum expansion factor in the vertical direction.

Grid	Nodes	Δx, Δy	$\Delta z_{\rm min}$	$f_{z_{\rm max}}$
Coarse	$96\times48\times68$	2.00	0.200	1.10
Medium	$136\times68\times96$	1.41	0.141	1.07
Fine	$192\times96\times136$	1.00	0.100	1.05

Forest Edge

Physical Domain and Boundary Conditions

For the flow across a forest edge, the configuration of Yang *et al.* (2006*a*) was considered: a computational domain with 288 m $\times$ 144 m $\times$ 46.5 m in the streamwise, spanwise and vertical directions. The forest was located in the lower 7.5 m of the domain and is 144 m long. Boundary conditions were similar to the homogeneous canopy, except that the ground roughness was $z_0 = 2.8$ cm and the average wind speed was $U_b = 3$ m/s.

Two reference simulations were also performed: one for the flow over a forest that occupies the full length of the domain and another for a simple boundary-layer flow, without forest.

Grid Results will be presented using a single grid, with $384\times192\times71$ nodes and resolution $\Delta x = \Delta y = 0.75$ m and $\Delta z_{\rm min} = 0.15$ m. This grid had the same resolution $\Delta x/h_{\rm can}$ and $\Delta y/h_{\rm can}$ as the fine grid of the homogeneous canopy and, to limit the computational resources used, $\Delta z_{\rm min}/h_{\rm can}$ was the same as the homogeneous canopy coarse grid.

VALIDATION

To assess numerical uncertainty, a comparison of results obtained using the different grids and the various LAI considered in the homogeneous canopy flow was done. Figure 1 shows comparisons of mean velocity, resolved turbulent kinetic energy and shear stress profiles for $LAI = 5$ with results from SS92. $LAI = 5$ was chosen because it is the case with more results available and is also the most demanding, since drag forces are larger. Turbulent kinetic energy and shear stress are normalized by the friction velocity, calculated using the total shear stress at the canopy top (resolved and subgrid).

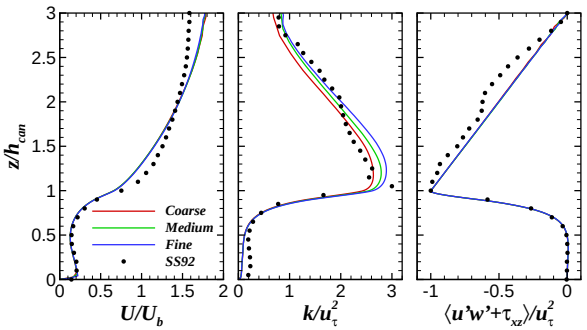

Figure 1. Mean velocity profiles, resolved turbulent kinetic energy and total shear stress (resolved and subgrid) with $LAI = 5$ obtained with different grids, compared with results from Shaw & Schumann (1992).

The mean velocity and the normalized shear stresses showed grid independence while, above the canopy, the resolved turbulent kinetic energy increased with grid resolution (+10% in peak value between coarse and fine grids). Maximum shear also increased around 10% at the canopy top, which provides an indication about the uncertainty associated with grid resolution: doubling the grid did not change first order quantities but resolved turbulence increased roughly 10%.

There are differences between our results and those of SS92 in the mean velocity profile above the canopy top and the shape of the turbulent kinetic energy peak (smooth vs. sharp) that we attributed to the coarser grid resolution in the vertical direction of the SS92 simulations. Differences in the shear

stress are due to the smaller sample size of SS92, that averaged only across homogeneous directions for a single time, while our results are averaged across time and homogeneous directions. Regarding the differences in the turbulent kinetic energy in the lower part of the canopy ($z/h_{\rm can} < 0.5$), it is likely related to differences in the wall-stress or subgrid models.

RESULTS AND DISCUSSION

The homogeneous canopy flow will be first considered and coefficients for the RaNS $k-\varepsilon$ canopy model will be devised. Then, the validity of the conclusions will be assessed in the more complex configuration that is the flow across the forest edge.

Homogeneous Canopy

Mean Flow Comparing velocity, turbulent kinetic energy and shear stress profiles for various *LAI* shows an expected reduction of all the quantities inside the canopy with increased foliage density (figure 2), due to the higher drag. Above the canopy, mass conservation implies that higher *LAI* corresponds to higher velocities, while normalized turbulent kinetic energy showed similar peak values.

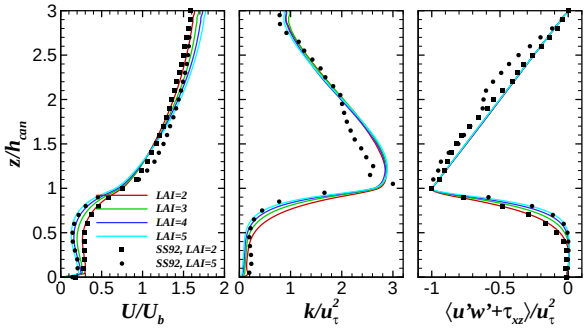

Figure 2. Mean velocity profiles, resolved turbulent kinetic energy and total shear stress (resolved and subgrid) obtained with different leaf area indices.

Turbulent Kinetic Energy Budgets In order to improve RaNS $k-\varepsilon$ models, we considered the transport equation for the resolved turbulent kinetic energy (k),

$$\frac{\partial k}{\partial t} = \mathscr{C}_k + \mathscr{P}_k - \varepsilon + \mathscr{T}_k + \mathscr{S}_k \,, \tag{4}$$

where

$$\mathscr{C}_k = -\langle U_j \rangle \frac{\partial k}{\partial x_j} \,, \tag{5}$$

$$\mathscr{P}_k = -\langle u_i' u_j' \rangle \frac{\partial \langle U_i \rangle}{\partial x_j} \,, \tag{6}$$

$$\varepsilon = \nu \left\langle \frac{\partial u_i'}{\partial x_j} \frac{\partial u_i'}{\partial x_j} \right\rangle - \left\langle \tau_{ij}' \frac{\partial u_i'}{\partial x_j} \right\rangle \,, \tag{7}$$

$$\mathscr{T}_k = -\frac{\partial}{\partial x_j} \left[\frac{1}{2} \langle u_i' u_i' u_j' \rangle + \langle \tau_{ij}' u_i' \rangle + \frac{1}{\rho} \langle p' u_j' \rangle - \nu \frac{\partial k}{\partial x_j} \right] \,, \tag{8}$$

$$\mathscr{S}_k = -C_z \left\langle |\overline{\mathbf{u}}| \overline{u}_i u_i' \right\rangle \tag{9}$$

are the mean convection, production, dissipation, turbulent transport and the canopy drag action ($C_z = C_d\, a(z)$). The subgrid stresses contribute to both the turbulent transport (8) and to the dissipation (7).

In the case of the homogeneous canopy, the mean convection (5) is zero. An analysis of the remaining terms in (4) showed that canopy drag contribution (9) is always negative, i.e. it destroys k (figure 3). For $z/h_{\rm can} < 0.8$, it is balanced by turbulent transport; above, it is balanced by production. Note that the peak production near the canopy top, due to simultaneous high shear and shear-stress, is a consequence of the canopy, but not the result of a direct action. The higher *LAI* increases the peak values and makes them narrower, but does not affect the relative contributions. As Finnigan (2000) finds, turbulence inside the canopy is far from local equilibrium: turbulent transport is positive for $z/h_{\rm can} < 0.9$, showing that turbulence inside the canopy is mainly transported from above. The subgrid model dominates the dissipation, but contributes less than the turbulent convection and the pressure to the turbulent transport.

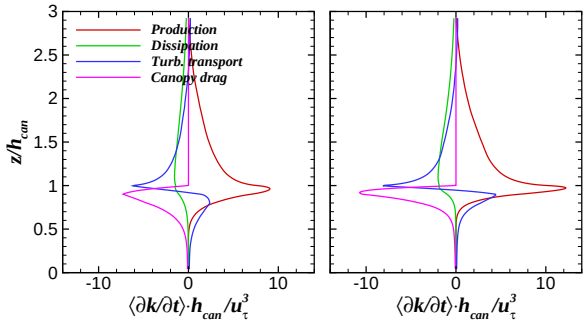

Figure 3. Turbulent kinetic energy budgets for $LAI = 2$ and 5. Dissipation and turbulent transport include contributions from both resolved and subgrid fields.

The budget of the dissipation of turbulent kinetic energy (ε) was also analyzed, even if resolved dissipation is almost always less than 1% of the total dissipation. Resolving a significant part of the dissipation in an atmospheric flow with the scales considered here (canopy height) is beyond the possibilities of the available computational resources. The transport equation for the dissipation of turbulent kinetic energy includes several terms that we do not detail here. Since our main interest is on the effect of the canopy drag and how it is balanced, we consider a production, which has origin on the non-linear terms of the Navier-Stokes equations, a dissipation,

due to the subgrid stresses, and the canopy effect,

$$\mathscr{S}_\varepsilon = -\left\langle \frac{\partial}{\partial x_j}\left(C_z|\overline{\mathbf{u}}|\overline{u}_i\right)\cdot\frac{\partial u_i'}{\partial x_j}\right\rangle . \qquad (10)$$

The canopy drag acted also as a sink for the resolved dissipation of turbulent kinetic energy (figure 4). However, unlike the turbulent kinetic energy budget, it did not dominate the destruction and is of the same order or less than the effect of the subgrid model. The contribution of the pressure and the viscous stresses was much smaller than the other terms.

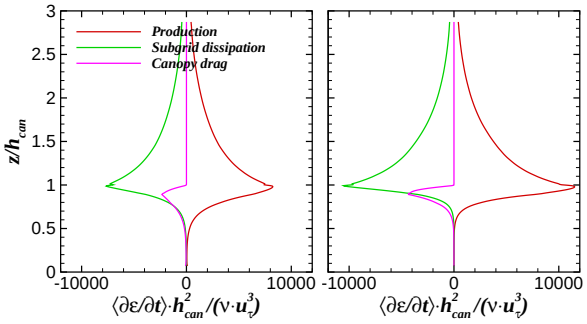

Figure 4. Dissipation of turbulent kinetic energy budgets for $LAI = 2$ and 5.

RaNS $k-\varepsilon$ Modeling Modeling the canopy effect in the turbulence with RaNS $k-\varepsilon$ models requires estimating $\mathscr{S}_k$ (9) and $\mathscr{S}_\varepsilon$ (10) using only the mean-flow velocity, the turbulent kinetic energy and its dissipation. The models available (e.g. Katul *et al.*, 2004; Sogachev & Panferov, 2006) have the general form (model 1)

$$\mathscr{S}_k^{k-\varepsilon} = C_z\left(\beta_p|\mathbf{U}|^3 - \beta_d|\mathbf{U}|k\right) ,$$
$$\mathscr{S}_\varepsilon^{k-\varepsilon} = C_z\left(C_{\varepsilon 4}\beta_p\frac{\varepsilon}{k}|\mathbf{U}|^3 - C_{\varepsilon 5}\beta_d|\mathbf{U}|\varepsilon\right) ,$$

where β_p, β_d, $C_{\varepsilon 4}$ and $C_{\varepsilon 5}$ are coefficients whose values change according to authors' proposals. β_p represents the fraction of mean flow kinetic energy converted to wake-generated k by canopy drag (a source term) and β_d is the fraction of k dissipated by short-circuiting of the energy cascade (a sink term). Terms in the ε transport equation have little physical basis, beyond dimensional arguments (Sanz, 2003).

One of the goals of this work is to find appropriate values for the coefficients β_p, β_d, $C_{\varepsilon 4}$ and $C_{\varepsilon 5}$ using results from the large-eddy simulations and the least squares method. To draw valid conclusions using the resolved dissipation, which is much smaller than the total dissipation, we have to consider that the effect of the canopy drag in the dissipation budget is proportional to the dissipation itself. This seems a reasonable assumption, since it is already used in the $k-\varepsilon$ model for the production and destruction terms. In addition, it adds an alternative approach to a subject where dimensional arguments prevail.

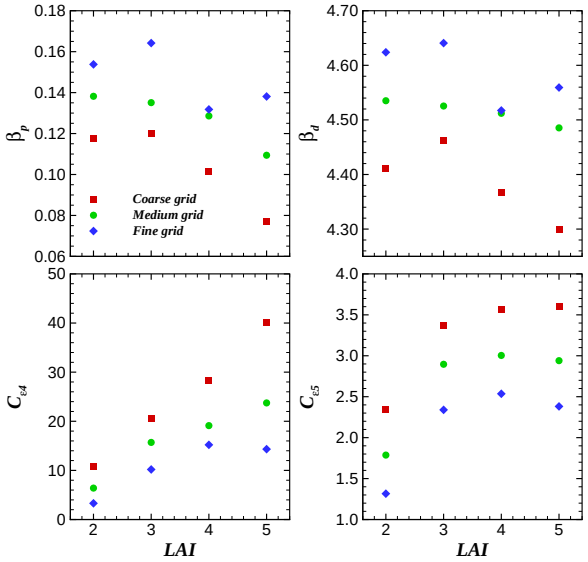

Figure 5. RaNS $k-\varepsilon$ canopy model 1 coefficients function of the *LAI* for each grid resolution.

The coefficients depend on grid resolution, which is expected since the least squares method uses second-order quantities that have the same dependence (figure 5). However, the coefficients depend as much on the leaf area index, which is undesirable when the goal is to have a simple model that should consider the *LAI* effect only through C_z. The quality of the fit is good for the effect of the canopy in the turbulent kinetic energy (figure 6): considering all the grids and all the *LAI*, the maximum error is 70%, near the ground, where $\mathscr{S}_k$ approaches zero; for $z/h_{\mathrm{can}} > 0.4$, the error was always lower than 30%. Regarding the dissipation of turbulent kinetic energy, the error is maximum near the ground, but even for $z/h_{\mathrm{can}} > 0.4$ it can be larger than 100%. Another problem of the $\mathscr{S}_\varepsilon$ model is that it predicted positive values near the ground, whereas the large-eddy simulations showed that the effect of the canopy was always destroying both turbulent kinetic energy and its dissipation.

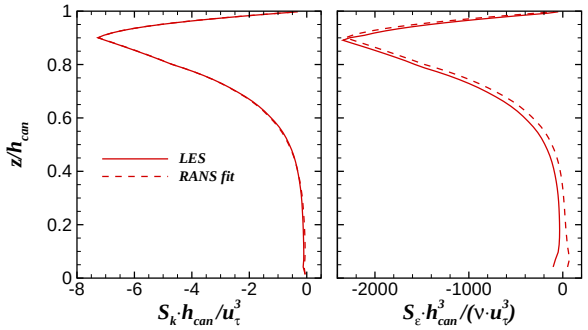

Figure 6. Comparison between large-eddy simulation results and RaNS $k-\varepsilon$ fit with model 1 for the canopy effect of turbulent kinetic energy and its dissipation ($LAI = 2$).

The "sink" effect of the canopy is not a surprise: in-

creased turbulent production occurs at the foliage scale and is due, for instance, to horizontal heterogeneity (Finnigan, 2000). As such, it cannot be reproduced in our large-eddy simulations. However, such small-scale motions dissipate quickly and contribute little to the turbulent kinetic energy (Shaw *et al.*, 1988). As a result, one can argue that the "sink" effect of the canopy in the turbulent kinetic energy and its dissipation should be enforced in the RaNS $k-\varepsilon$ model, which can be done with a model with only a negative part and two coefficients (model 2),

$$\mathscr{S}_k^{k-\varepsilon} = -C_z \beta_d |\mathbf{U}| k \,,$$
$$\mathscr{S}_\varepsilon^{k-\varepsilon} = -C_z C_{\varepsilon 5} \beta_d |\mathbf{U}| \varepsilon \,.$$

The uncertainty associated with the determination of the model coefficients by the least squares method was smaller for model 2 than for model 1, considering the range of values obtained for the different grid resolutions and *LAI*, especially for $C_{\varepsilon 5}$. The fit also showed smaller relative errors with model 2: in the turbulent kinetic energy, the error was always smaller than 25% and in the turbulent kinetic energy dissipation it is larger then 20% only for $z/h_{\mathrm{can}} > 0.9$ (figure 8).

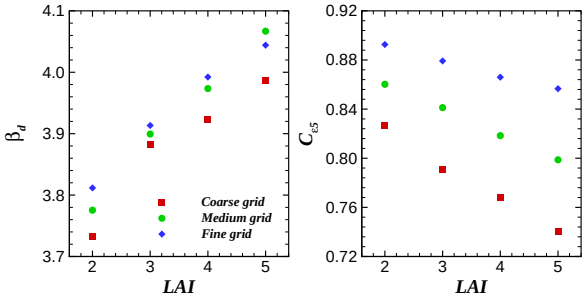

Figure 7. RaNS $k-\varepsilon$ canopy model 2 coefficients function of the *LAI* for each grid resolution.

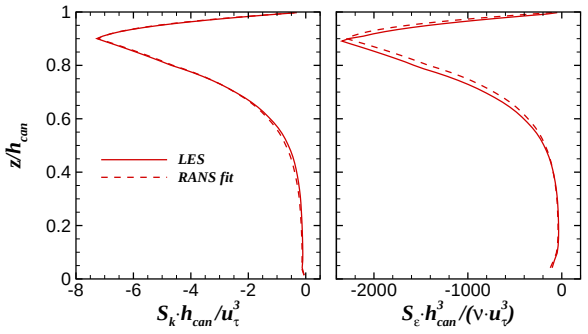

Figure 8. Comparison between large-eddy simulation results and RaNS $k-\varepsilon$ fit with model 2 for the canopy effect of turbulent kinetic energy and its dissipation ($LAI = 2$).

Considering that the least squares method usually provided higher values for β_d and $C_{\varepsilon 5}$ when higher grid resolutions were used and that, in practical cases, we find more frequently lower leaf area indexes, our proposal of values for the model 2 coefficients is $(\beta_d, C_{\varepsilon 5}) = (4.0, 0.9)$. These values were already suggested for RaNS $k-\varepsilon$ canopy models (Green, 1992; Liu *et al.*, 1996; Sanz, 2003), but here it is the first time they are associated in a model with only a negative part.

Forest Edge

The objective of the simulation of the flow across a forest edge is to test the applicability of the canopy model derived from the results of the homogeneous canopy to a slightly more complex configuration. The mean flow is no longer only horizontal, there are pressure gradients besides the required to balance the wall-stress and the canopy effect depends not only on the distance to the ground but also on the distance to the edge.

A comparison of the mean velocity profiles between our results and those of Yang *et al.* (2006*a*) showed some differences for $z/h_{\mathrm{can}} > 2$, most likely due to different forcing: our flow was driven by a pressure gradient, while Yang *et al.* (2006*a*) applied a force for $z/h_{\mathrm{can}} \geq 5$, which is transmitted down by the shear-stress. Also, when entering the forest, the flow seems to decelerate slightly slower near the ground in our simulation, which can be caused by a different wall-stress condition. Comparing with the long forest, we can see that by $x/h_{\mathrm{can}} = 14.5$ the mean velocity profile is almost completely developed. It is near the ground that the flow takes longer to develop, probably because of the lower drag force there.

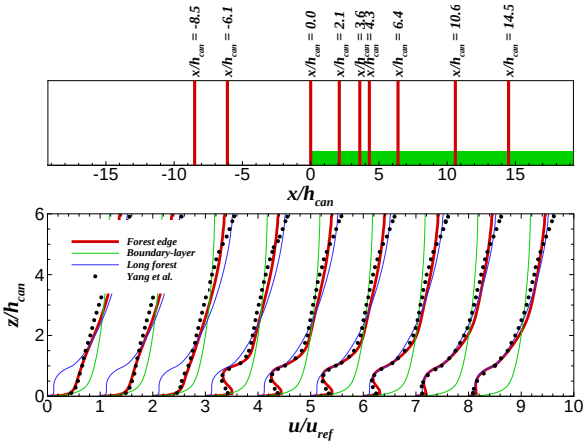

Figure 9. Streamwise velocity profiles in the forest edge flow, compared with long forest, boundary-layer and Yang *et al.* (2006*a*) results.

A comparison between canopy models 1 and 2 in the forest edge flow showed a better approximation with model 2, as in the homogeneous canopy. The maximum error with both models is similar, for both turbulent kinetic energy and dissipation budgets, but errors larger than 40% are rare with model 2, while they exist in zones longer than h_{can} with model 1. However, the most relevant comparison is with the coefficients of each model: whereas the coefficients for model 1 were highly case dependent, the coefficients for

model 2 were similar to the values obtained in the homogeneous canopy flow and for the long forest with the same configuration (table 2).

Table 2. Least squares fit of canopy model coefficients to the large-eddy simulation results.

Model 1

	β_p	β_d	$C_{\varepsilon 4}$	$C_{\varepsilon 5}$
Long forest	0.018	4.18	310.7	5.73
Forest edge	0.073	4.31	0.53	0.75

Model 2

	β_d	$C_{\varepsilon 5}$
Long forest	4.11	0.68
Forest edge	3.80	0.79

The coefficients listed in table 2 are the "best" (in a least squares sense) for the whole forest, but not necessarily the "best" at each vertical section. Not surprisingly, during the initial length the coefficients can change significantly (figure 10) and the model overpredicts the effect of the canopy on both k and ε budgets. However, after $x/h_{\rm can} \approx 5$ they approach the values for a long forest.

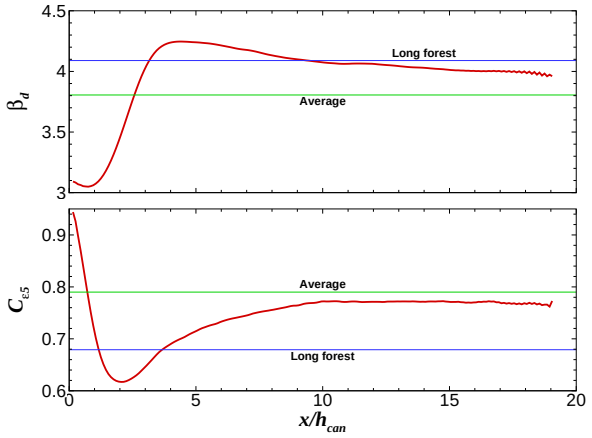

Figure 10. Evolution of model 2 coefficients along the forest in the forest edge flow.

As a final comment, the values found here for $C_{\varepsilon 5}$ are lower than what was proposed based on the homogeneous canopy flow. Further studies should check the reason of this discrepancy and see if, for instance, it was due to the lower vertical resolution of the grid.

CONCLUSIONS

Large eddy simulations of the flow over a long forest were used to find coefficients for a RaNS $k-\varepsilon$ canopy model. The results showed that the effect of the drag force due to the forest was destroying both the turbulence kinetic energy and its dissipation. As such, an appropriate canopy model can be $\mathscr{S}_k^{k-\varepsilon} = -C_z\beta_d|\mathbf{U}|k$, $\mathscr{S}_\varepsilon^{k-\varepsilon} = -C_zC_{\varepsilon 5}\beta_d|\mathbf{U}|\varepsilon$, with $(\beta_d, C_{\varepsilon 5}) = (4.0, 0.9)$. *A priori* test of this model showed errors usually lower than 25%, which seems appropriate for the $k-\varepsilon$ turbulence model.

In the case of the flow across a forest edge, it was found that it overestimates the effect of the canopy on both turbulent kinetic energy and dissipation budgets in the initial part of the forest (with length about five times the tree height), but then approaches the accuracy obtained in the long forest.

REFERENCES

Finnigan, J.J. 2000 Turbulence in plant canopies. *Annual Review of Fluid Mechanics* **32**, 519–571.

Green, S.R. 1992 Modelling turbulent air flow in a stand of widely-spaced trees. *The PHOENICS Journal of Computational Fluid Dynamics and its Applications* **5**, 294–312.

Katul, G.G., Mahrt, L., Poggi, D. & Sanz, C. 2004 One- and two-equation models for canopy turbulence. *Boundary-Layer Meteorology* **113**, 81–109.

Liu, J., Chen, J.M., Black, T.A. & Novak, M.D. 1996 $E-\varepsilon$ modelling of turbulent air flow downwind of a model forest edge. *Boundary-Layer Meteorology* **77**, 21–44.

Marusic, I., Kunkel, G.J. & Porté-Agel, F. 2001 Experimental study of wall boundary conditions for large-eddy simulation. *Journal of Fluid Mechanics* **446**, 309–320.

Mason, P.J. & Thomson, D.J. 1992 Stochastic backscatter in large-eddy simulations of boundary layers. *Journal of Fluid Mechanics* **242**, 51–78.

Meneveau, C., Lund, T.S. & Cabot, W.H. 1996 A Lagrangian dynamic subgrid-scale model of turbulence. *Journal of Fluid Mechanics* **319**, 353–385.

Sanz, C. 2003 A note on $k-\varepsilon$ modelling of vegetation canopy air-flows. *Boundary-Layer Meteorology* **108**, 191–197.

Shaw, R.H., Hartog, G. & Neumann, H.H. 1988 Influence of foliar density and thermal stability on profiles of Reynolds stress and turbulence intensity in a deciduous forest. *Boundary-Layer Meteorology* **45**, 391–409.

Shaw, R.H. & Schumann, U. 1992 Large-eddy simulation of turbulent flow above and within a forest. *Boundary-Layer Meteorology* **61**, 47–64.

Silva Lopes, A., Palma, J.M.L.M. & Castro, F.A. 2007 Simulation of the Askervein flow. Part 2: large-eddy simulations. *Boundary-Layer Meteorology* **125**, 85–108.

Sogachev, A. & Panferov, O. 2006 Modification of two-equation models to account for plant drag. *Boundary-Layer Meteorology* **121**, 229–266.

Yang, B., Raupach, M.R., Shaw, R.H., Paw U, K.T. & Morse, A.P. 2006*a* Large-eddy simulation of turbulent flow across a forest edge. Part I: Flow statistics. *Boundary-Layer Meteorology* **120**, 377–412.

Yang, B., Morse, A.P., Shaw, R.H. & Paw U, K.T. 2006*b* Large-eddy simulation of turbulent flow across a forest edge. Part II: Momentum and turbulent kinetic energy budgets. *Boundary-Layer Meteorology* **121**, 433–457.